EphrinB2 coordinates the formation of a morphological boundary and cell epithelialization during somite segmentation

Tadayoshi Watanabe[a], Yuki Sato[a,b,1], Daisuke Saito[a], Ryosuke Tadokoro[a], and Yoshiko Takahashi[a,2]

[a]Graduate School of Biological Sciences, Nara Institute of Science and Technology, 8916-5, Takayama, Ikoma, Nara 630-0192, Japan; and [b]Center for Developmental Biology, RIKEN, 2-2-3 Minatojima Minami, Chuou-ku, Kobe 650-0047, Japan

Communicated by N. M. Le Douarin, Collège de France, Paris, France, March 17, 2009 (received for review September 5, 2008)

During early morphogenesis, tissue segregation is often accompanied by changes in cell shape. To understand how such coordination is regulated, somitogenesis was used as a model. When a somite forms in the anterior end of the presomitic mesoderm, an intersomitic boundary (gap) emerges, and it is rapidly followed by cell epithelialization at this border. It has been known that the gap formation is regulated by intercellular signals. We here demonstrate that cMeso-1, the chicken homolog of mouse Mesp2, up-regulates EphA4 in the cells located posteriorly to a forming boundary. This in turn activates EphrinB2-reverse signals in the anteriorly juxtaposed cells, where the EphrinB2 signal is sufficient to cause a gap formation and cell epithelialization cell-autonomously. During these processes, Cdc42 needs to be repressed via tyrosine phosphorylation of EphrinB2. This is the first demonstration that Ephrin-reverse signal acts as a platform that couples distinct morphogenetic changes in cell polarity and tissue shape.

Ephrin | Epithelialization | Segmentation

During early development, a segregation from a homologous group of cells into distinct types of cell populations is a basis for morphogenesis producing a variety of tissues and organs. Formation of a morphological boundary within a continuous tissue is a typical strategy to achieve the segregation. In addition, such a boundary is often associated with dynamic changes in cell morphology, i.e., a transition between epithelial and mesenchymal states of cells. Although molecular mechanisms underlying intercellular and intracellular regulation of epithelial cells have extensively been studied, how changes in cell shape are coordinated with a construction of three dimensional tissues remains largely unknown.

Somitogenesis, which proceeds periodically and repetitively in early vertebrate embryos, has been used as a model to study the molecular and cellular mechanisms underlying morphological segregation and boundary formation. In addition, the formation of an intersomitic boundary (gap) occurs concomitantly with a mesenchymal-to-epithelial transition (MET) of cells that face a forming gap. It was previously shown that cells at the site of next-forming boundary in the presomitic mesoderm (PSM) become specified to act on their anteriorly positioned cells to make a morphological gap (1, 2). However, it remains unsolved at the molecular and cellular levels how the intersomitic gap is induced to form and how the gap formation is coordinated with the MET.

For the formation of intersomitic gap, it was shown by murine genetics that the bHLH-transcription factor MesP2, expressed at the next-forming boundary, is essential (3). Analyses of chimeric embryos between MesP2$^{+/+}$ and MesP2$^{-/-}$ also implied that MesP2-expressing cells influence neighboring cells to become epithelial (4). In addition, *MesP2* requires Notch signals to start its expression in PSM (5), and Notch activation is sufficient for the formation of an ectopic gap (1). Furthermore, when the MET occurs concomitantly with the gap formation, the Rho-family member Cdc42 is known to be critical for the epithelialization of cells that are juxtaposed to the forming gap (6). In this study we have clarified the molecular cascade originating from the *MesP* gene in posterior border cells to the Cdc42-mediated MET of anterior border cells through intercellular signaling. We have found that an anteroposteriorly asymmetric activation of Ephrin-reverse signaling acts as a platform that couples the distinct morphogenetic changes in cell polarity and tissue shape in a cell autonomous manner.

Results and Discussion

cMeso-1 Is Sufficient to Induce a Gap Formation. We started our study to clarify the action of cMeso-1, the chicken homolog of mouse MesP2, by using the gap-inducing assay that we established previously (1) (Fig. 1*A* and *B*). Briefly, the gene(s) to be examined is electroporated into the presumptive somite of a donor embryo before the ingression of mesoderm (at the primitive streak stage), and subsequently a piece of electroporated PSM is dissected and transplanted into a normal host PSM to see if this manipulation would result in the formation of an ectopic gap. However, we were confronted with a problem that *cMeso-1*-electroporated cells failed to ingress from the primitive streak in the donor embryo, probably because cMeso-1 also plays a role in the ingression process (7, 8). We therefore circumvented this problem by applying the tetracycline-inducible expression (tet-on) method that we have recently optimized for chickens (7) (for details, see Fig. 1*B* and Materials and Methods). Embryos of stage 8 were co-electroporated with pTRE-cMeso1-EGFP (TRE, bidirectional promoter including the tet-responsive element), pCAGGS-rtTA2^{s}-M2 (rtTA2^{s}-M2, tet-dependent activator bound to TRE), and pCAGGS-DsRed-E, followed by a transplantation into a host embryo. Whereas signals of EGFP remained negative without Dox (analog of tetracycline), they turned on soon after Dox administration (Fig. 1*B*). Thus, an expression boundary of *cMeso-1* was successfully created in PSM at the site that would normally not segment (level −1.5, Fig. 1*B*), making a gap-inducing assay available. We found that this manipulation resulted in the formation of an ectopic gap that demarcated the expression area of introduced *cMeso-1* (n = 44; Fig. 1*C*). Two types of control experiments did not yield such a gap formation (TRE-EGFP with Dox, n = 45; TRE-cMeso1-EGFP without Dox, n = 10) (Fig. 1*C*).

EphA4 Is Up-Regulated by cMeso-1 and Activates EphrinB2-Reverse Signals in the Anteriorly Juxtaposed Cells. We next asked what molecules acted downstream of cMeso-1 to form the gap by

Author contributions: Y.S. and Y.T. designed research; T.W., Y.S., D.S., and R.T. performed research; T.W., Y.S., R.T., and Y.T. analyzed data; D.S., and R.T. contributed new reagents/analytic tools; and T.W. and Y.T. wrote the paper.

The authors declare no conflict of interest.

[1]Present address: California Institute of Technology, Biological Imaging Center, 1200E, Beckman Institute, Pasadena, CA 91125.

[2]To whom correspondence should be addressed. E-mail: yotayota@bs.naist.jp.

This article contains supporting information online at www.pnas.org/cgi/content/full/0902859106/DCSupplemental.

DEVELOPMENTAL BIOLOGY

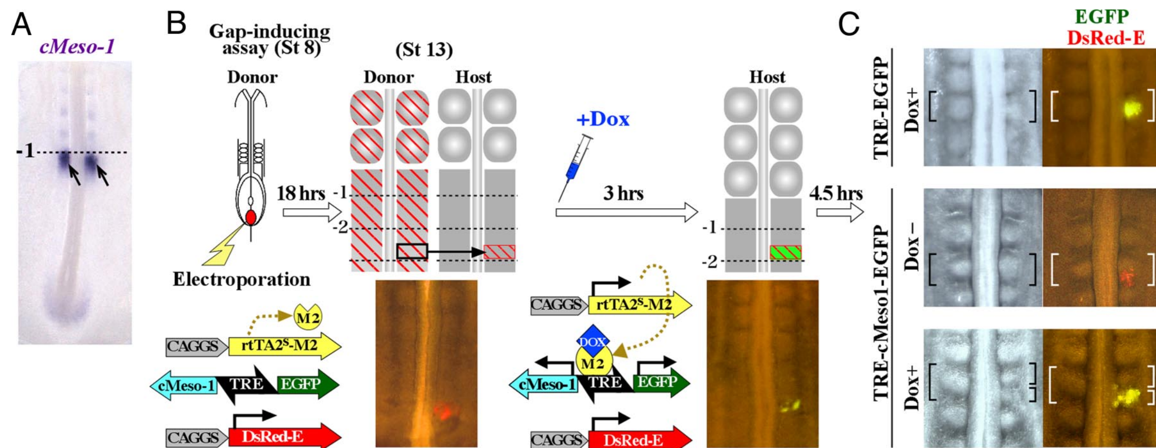

Fig. 1. An ectopic boundary was induced to form at the interface of cMeso-1 expression. (*A*) In a normal embryo, a *cMeso-1* positive region coincides with the next-forming boundary. (*B*) The gap-inducing assay. DNA plasmids are electroporated into the presumptive somitic mesoderm of stage 8 embryos before these cells ingress. After 18 hours, a piece of transgenic PSM dissected from a donor embryo is transplanted into a non-electroporated embryo at the site that would normally not segment (level −2.5). Because *cMeso-1* overexpression prevented the mesodermal ingression, the tet-on inducible expression system was used in this study. TRE-cMeso1-EGFP remained inactive before the Dox injection enabling the mesodermal ingression. Expression of cMeso-1 and EGFP starts by injecting Dox when a donor tissue was transplanted. (*C*) When assessed at 4.5 hours posttransplantation, only the cells turning on cMeso-1 (and EGFP) could produce an ectopic boundary. Control specimens treated similarly using either pTRE-cMeso1-EGFP without DOX, or pTRE-EGFP with DOX yielded no formation of ectopic boundary.

focusing on five different genes expressed at level −1; *EphA4*, *Sox9*, *PAPC*, *Pax2*, *and Tbx18* (Fig. 2*A*). Expression of all these genes except *Tbx18* was found to be up-regulated by overexpression of *cMeso-1* [supporting information (SI) Fig. S1]. We therefore performed a gap-inducing assay for each of the four genes (Fig. S1, Fig. 2*D*), and found that only EphA4 was capable

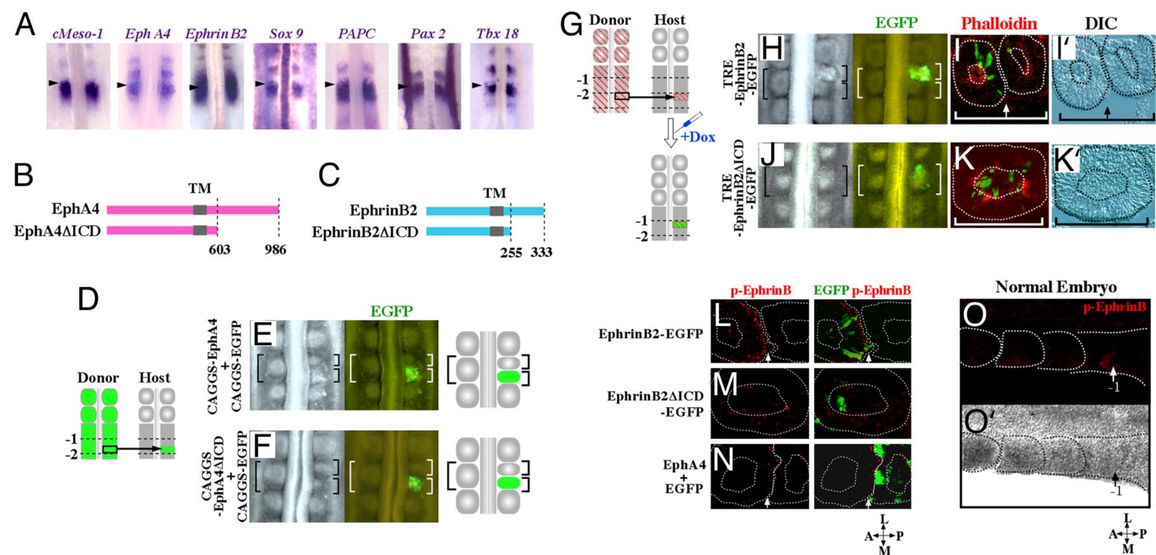

Fig. 2. Eph-Ephrin signals are sufficient to induce a formation of ectopic boundary. (*A*) Whole-mount *in situ* hybridization to show expression patterns of *cMeso-1*, *EphA4*, *EphrinB2*, *Sox9*, *PAPC*, *Pax2*, and *Tbx18* in the anterior end of PSM of E2 embryos. An arrowhead shows a level of next-forming boundary (level −1). (*B* and *C*) Schematic structures of EphA4 and EphrinB2 molecules, and their mutant forms lacking the cytoplasmic region. TM, transmembrane region. (*D*) For the gap-inducing assay using EphA4 or its mutant, a piece of electroporated PSM was transplanted into the posterior half of a somitic unit (compare with *G*). (*E* and *F*) Photographs of bright and dark fields show a dorsal view of the same embryo. (*G*) For the gap-inducing assay using EphrinB2 and its mutant, a piece of electroporated PSM was transplanted into the anterior half of a somitic unit (compare with *D*). As overexpression of EphrinB2 sometimes caused earlier effects during formation of PSM, the tet-on method was used as shown in Fig. 1. (*H* and *I*) EphrinB2-electroporated cells were capable of forming an ectopic gap. (*H*) Dorsal views of manipulated embryos (anterior to the top). Some of these embryos were whole-mount stained with phalloidin, and confocal images of horizontal view over a 10-μm thickness were obtained (*I*, anterior to the left and midline to the bottom; neural tube discarded). The same specimens were further subjected to paraffin-sectioning to obtain the same view for Nomarski microscopy (*I′*). Most of EphrinB2-electroporated cells resided in the epithelial component of a formed somite. An arrow indicates a gap ectopically formed. (*J* and *K*). EphrinB2ΔICD-electroporated cells failed both to induce a gap (*J*) and to correctly epithelialize (*K* and *K′*). (*L*–*N*) Manipulated somites were stained with anti–phospho-EphrinB antibody and confocal images of horizontal view over a 10-μm thickness were obtained (anterior to the left and midline to the bottom; arrow indicates an ectopic gap). EphrinB2-electroporated cells (green) anteriorly positioned to the ectopically formed gap were positively stained (red in *L*), whereas cells with EphrinB2ΔICD were not (*M*). (*N*) When an ectopic gap was formed by *EphA4*-electroporated cells (green), non-electroporated cells positioned anteriorly were stained for phospho-EphrinB. (*O*) Activation of EphrinB-reverse signaling in the anterior PSM of normal embryos, visualized by staining with anti-phospho-EphrinB antibody. Signals were restricted to the cells located anteriorly to a forming boundary (−1). Confocal image of horizontal view over a 10-μm thickness was obtained (anterior to the left and midline to the bottom; neural tube discarded.

of inducing an ectopic gap (n = 19, Fig. 2*E*, Fig. S1, Fig. S2*A*). *Pax2* was shown to play a role in cell condensation in PSM before the gap formation (7).

It is known that when Eph- and Ephrin-expressing cells interact, either an Eph-forward signal or an Ephrin-reverse signal, or both, are activated. We therefore investigated which of them is essential for the induction of intersomitic gap formation. We first used a mutant construct of *EphA4*, *EphA4ΔICD*, lacking the cytoplasmic region (Fig. 2*B*) to know whether the EphA4-derived forward signal was required. This mutant form was capable of inducing a gap formation (n = 10, Fig. 2*F*, Fig. S2B), suggesting that the forward signal is dispensable for this event.

We therefore reasoned that Ephrin activation in the cells that are anteriorly juxtaposed to the *EphA*4-expressing cells would be crucial for the gap-induction. To test this, we performed a gap-inducing assay using *EphrinB2*-electroporated PSM. In this case, a tissue piece dissected from an electroporated donor PSM was transplanted into the anterior half of a presumptive somite (compare Fig. 2*G* with 2*D*). EphrinB2 was found to be sufficient to induce a formation of ectopic gap (Fig. 2 *H* and *I*, n = 10). Moreover, a removal of the cytoplasmic region of EphrinB2 (EphrinB2ΔICD, Fig. 2*C*) abrogated the inductive action of this protein (Fig. 2 *J* and *K*; n = 12), indicating that the reverse signal derived from EphrinB2 is critical for the formation of intersomitic gap.

It is known that the cytoplasmic region of Ephrin molecules undergoes phosphorylation when activated to transduce reverse signals intracellularly. To see whether the EphrinB2-electrporated cells that were capable of the gap-induction were activated for the reverse signal, anti-phospho-EphrinB antibody was used for immunohistochemistry. Phosphorylation signals were detected in the EphrinB2-electroporated cells facing the ectopically formed gap (Fig. 2L). In contrast, such signals were not observed in the cells electroporated with EphrinB2ΔICD (Fig. 2M). In addition, when an ectopic gap was formed by EphA4-electroporated cells, the anteriorly located non-electroporated cells also exhibited Ephrin-phosphorylation signals (Fig. 2N). Thus, the ectopically formed gap appears to be caused by the activation of EphrinB2-reverse signals. Furthermore, staining of a PSM of normal embryos with anti-phospho-EphrinB antibody revealed a signal restricted to the cells anteriorly juxtaposed to a forming gap (level −1) (n = 4; Fig. 2*O*), supporting the notion that EphrinB2-reverse signals play an important role in the formation of a morphological boundary during normal somitogenesis. During this series of analyses we also noticed cell morphology affected by EphrinB2 or its mutant form (Fig. 2 *I* and *K*). The role for EphrinB2 in the shaping of somitic cells is demonstrated below with more experimental evidence.

We further explored the intracellular signals directed by EphrinB2. The PDZ-binding (PDZb) domain at the C terminus and possible phosphorylation of three tyrosine residues, at the positions of 304, 311, 316, have been implicated for the Ephrin-reverse signaling mainly using mammalian cultured cells (9, 10). We therefore made two mutant constructs: EphinB2ΔPDZb lacking the PDZb domain, and EphrinB2YF with the three tyrosine residues replaced by phenylalanines (Fig. 3*A*). We confirmed using the chicken cell line DF-1 that EphrinB2YF failed to be phosphorylated when co-cultured with EphA4-expressing cells whereas a full length EphrinB2 was successfully phosphorylated (Fig. 3*B*).

Gap-inducing assays using these mutant constructs revealed that EphinB2 ΔPDZb (Fig. 3*C*, n = 11), but not EphrinB2YF (Fig. 3*E*, n = 15), retained the gap-inducing activity, suggesting that the phosphorylation of the tyrosine residues is required for the gap induction whereas the PDZb domain is dispensable.

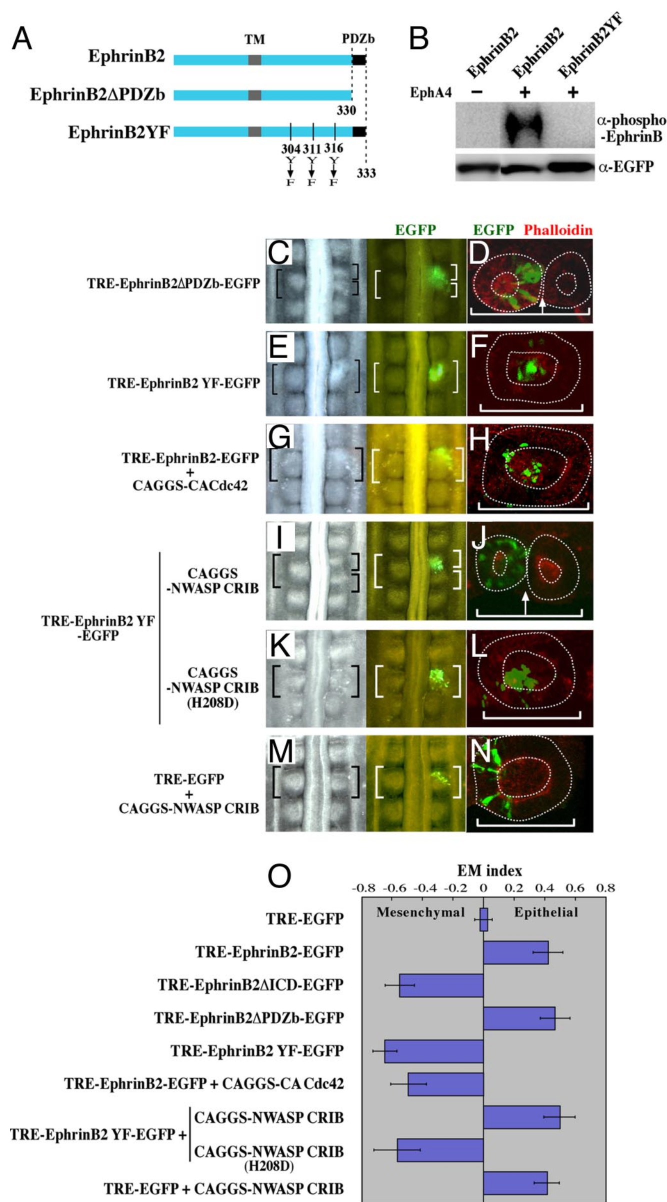

Fig. 3. Ephrin cell autonomously coordinates the gap formation and cell epithelialization through repression of Cdc42 activity. (*A*) A diagram showing mutant forms of EphrinB2. In the mutant EphrinB2YF, three tyrosine residues were replaced by phenylalanines. (*B*) Western blotting shows that the phosphorylation of EphrinB2 was dependent on interactions between EphA4 expressed in neighboring cells, and also that the phosphorylation was abrogated by the three Y-to-F replacements in the cytoplasmic region of EphrinB2. DF-1 cells that had been separately transfected with EphrinB2 and EphA4 were co-cultured and subjected to Western blotting to detect a phosphorylated form of Ephrin (see *Materials and Methods* for more details). (*C*, *E*, *G*, *I*, *K*, *M*) Dorsal views of host embryos subjected to a gap-inducing assay as shown in Fig. 2*G*. DNA plasmids used for the assay are indicated on the left. (*D*, *F*, *H*, *J*, *L*, *N*) Images of horizontal view over a 10-μm thickness obtained by confocal microscopy demonstrate epithelial or mesenchymal states of electroporated cells (green) in a formed somite. Anterior to the left and midline to the bottom. (*O*) A ratio between the numbers of epithelial and mesenchymal cells that received exogenous DNAs was compared using EM index as previously shown by Nakaya et al. (6). The number of epithelial cells was divided by the total number of electroporated cells in a given somite (E/E+M). This value (EM Index) was compared with that of EGFP control, which was set as zero.

EphrinB2 Coordinates the Gap Formation and Cell Epithelialization by Regulating Cdc42 Activity. During normal segmentation of somites in chicken embryos, a gap forms within the anterior area of

mesenchymal PSM, and this is soon followed by epithelialization of the cells that are *anteriorly* juxtaposed to the gap (the cells that are eventually positioned at the posterior edge of a formed somite). The cells *posteriorly* facing the gap (the cells that are eventually positioned at the anterior edge of a formed somite) undergo epithelialization at slightly later stages than the anterior cells (1). These MET processes following the gap formation produce a somite in which cells located in the outer layer are epithelial, whereas cells at the central position remain mesenchymal. These overt differences in position and shape between epithelial and mesenchymal cells within a single somite facilitate an assessment of effects on epithelialization of genetically manipulated cells (6).

Accordingly, the cells wherein EphrinB2-reverse signals are found to be activated (Fig. 2*O*) are the cells that also undergo MET concomitantly with the gap formation. It is postulated by *in vitro* studies that Ephrin-reverse signals regulate actin/cytoskeletal rearrangement (11). In addition, we previously reported that the MET-undergoing cells need to have a low level of Cdc42 (6). We therefore reasoned that EphrinB2-reverse signal coordinates the gap formation and MET by regulating the Cdc42 activity. To test this, we first examined a relationship between the gap-inducing ability and epithelial state of the cells using the series of *EphrinB2* mutant constructs as described above. In combination with the morphological assessments, a (immuno)-histochemical staining for phalloidin and N-cadherin was performed, which visualizes the apical lining that separates the epithelial layer from the mesenchymal population in a somite (Fig. 2 *I* and *K*, Fig. 3, Fig. S3).

A majority of the cells introduced with either full-length *EphrinB2* or *EprhinB2ΔPDZ*, both of which could confer the gap-forming activity, exhibited epithelial morphology (Figs. 2*I* and Fig. 3*D*, Fig. S3). By clear contrast, the cells introduced with either *Ephrin2BΔICD* or *EphrinB2YF*, the mutants incapable of gap-induction, remained mesenchymal at the center of a formed somite (Fig. 2 *K* and 3*F*, Fig. S3). Thus, a remarkable correlation between these distinct morphological events was found. The effects by *EphrinB2* constructs on the MET were quantitatively analyzed and compared using the EM index as previously reported (6) (Fig. 3*O*). Briefly, a proportion of the number of electroporated cells found in the epithelial component, positioned in the outer layer of a somite, was calculated over the total number of electroporated cells.

The intimate correlations between the gap-forming ability and epithelial cell state lead us to further investigate a regulation of Cdc42 activity by EphrinB2 during somitic boundary formation. We first activated Cdc42 experimentally using constitutively active form of Cdc42 (CA-Cdc42) (6) in the cells that were introduced with full-length *EphrinB2*, followed by a gap-inducing assay similar to that in Fig. 2*G*. This treatment abrogated the gap-forming activity of EphrinB2 (Fig. 3*G*, $n = 5$), suggesting that a low activity of Cdc42 is necessary for the gap-induction. Second, we tested whether the tyrosine phosphorylation of EphrinB2 was important for the repression of Cdc42 activity. Embryos were co-electroporated with *EphrinB2YF* and *NWASP-CRIB*, the latter widely used to block the endogenous activity of Cdc42 (12, 13), and subjected to the gap-inducing assay. This treatment restored the gap-inducing ability (Fig. 3*I*, $n = 6$), suggesting that in the gap-forming cells the EphrinB2-reverse signal suppresses the activity of Cdc42 through the tyrosine phosphorylation either directly or indirectly. The suppression by EphrinB2 appears to be specific to Cdc42 since *N-WASP-CRIB-H298D*, with a point mutation that prevents a binding of Cdc42 (6), failed to restore the gap-inducing activity when co-electroporated with *EphirnB2YF* (Fig. 3*K*, $n = 10$). Importantly, the restoration of the gap-forming ability of the cells co-electroporated with *EphrinB2YF* and *NWASP-CRIB* was accompanied with cell epithelialization (compare Fig. 3*J* with 3*F*). Such

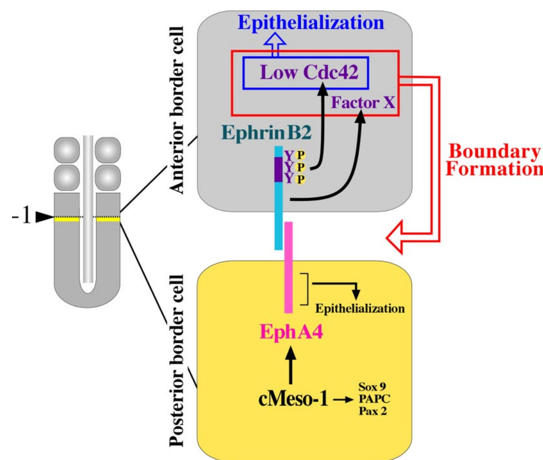

Fig. 4. Model showing how a coordination between the intersomitic gap formation and somitic cell epithelialization is regulated by the molecular cascade originating from transcriptional regulation by cMeso-1 to the Cdc42 regulation through intercellular signaling. In the border cells posterior to the next-forming boundary (yellow), cMeso-1 up-regulates *EphA4*, *Pax2*, *PAPC*, and *Sox9*, among which EphA4 is directly involved in the communication with the anterior border cells (gray). The Ephrin-reverse signal activated in the anterior border cells by EphA4 is sufficient to direct and couple the gap formation and cell epithelialization in a cell autonomous manner. For these events to occur, a repression of Cdc42 by EphrinB2 through tyrosine phosphorylation is required. In addition, an unidentified factor provided by EphrinB2-reverse signal is also needed for the gap formation, whereas lowering Cdc42 is sufficient for the cell epithelialization. The EphA4-forward signal is dispensable for the gap formation but is required for the self-epithelialization.

epithelialization did not occur in the cells co-electroporated with *EphrinB2YF* and *NWASP-CRIB-H298D* (Fig. 3*L*). Last, without the EphrinB2-reverse signal, a repression of Cdc42 activity failed to induce a gap formation (Fig. 3*M*, $n = 14$) although it was sufficient for the epithelialization as previously reported (6) (Fig. 3*N*). Taken together, these findings suggest that not only the phosphorylation of tyrosine residues but also other domains of the cytoplasmic region of EphrinB2 play a role in the gap-induction in conjunction of low activity of Cdc42.

In addition to the role of Ephrin-reverse signal in the MET of anterior border cells, we also noticed an effect by EphA4-forward signal on the MET process of the posterior border cells in a cell-autonomous manner. When the gap-inducing assay was performed using EphA4ΔICD, where an ectopic gap was successfully formed as shown earlier (Fig. 2*F*), the cells electroporated with this construct failed to undergo correct epithelialization (Fig. S2*B*, Fig. S3*D*). An assessment of EM-index for the cells electroporated with full-length EphA4 or EphA4ΔICD suggests that EphA4 appears to act positively for the epithelialization, for which the Eph-forward signal is required (Fig. S2, Fig. S3 *C* and *D*). During normal segmentation in chickens, the posterior border cells expressing *EphA4* undergo MET slightly later than the anterior border cells where an Ephrin-reverse signal is activated (this study). Thus, whereas Ephrin-reverse signals appear to be sufficient for the morphological boundary formation, bidirectional signals act in the opposing border cells for their own epithelialization. How the bidirectional signals are temporally regulated remains to be studied.

As shown in Fig. 4, we propose a model in which the molecular cascades are depicted that coordinate the formation of an intersomitic gap and the concomitantly occurring epithelialization of the cells during somitic segmentation. Step 1: cMeso-1 up-regulates *EphA4* in the cells located posteriorly to the next-forming boundary (yellow). Step 2: EphA4 interacts with EphrinB2 presented by the anteriorly juxtaposed cells (gray). The

reverse signals of EphrinB2 are transduced to repress the activity level of Cdc42 via tyrosine phosphorylation. The repression of Cdc42 is essential for directing at least two distinct outputs; cell epithelialization and gap formation. Although a low level of Cdc42 is sufficient for cell epithelialization as already shown by Nakaya et al. (6), it does not suffice to cause the gap formation (this study). It appears that an unidentified signal(s) provided by the intracellular region of EphrinB2 is required to cooperate with low Cdc42 in the cells to direct the intersomitic gap formation. It is yet to be studied how Ephrin-reverse signals regulate the Cdc42 activity in the anterior border cells. It is known in cultured cells that Grb4 acts as an SH2/SH3-adaptor that transduces the Ephrin-reverse signal to regulate Cdc42 (11). A chicken homolog of Grb4 is not, however, expressed in PSM (T. W. and Y. T., unpublished data). Step 3: After the epithelialization of anterior border cells, the posterior border cells (yellow) undergo MET, and EphA4-forward signal appears to be essential for this event.

In our study, cMeso-1 did not affect the expression of *Tbx18*, which was previously shown to possess a gap-inducing activity (14). It is conceivable that at least two distinct pathways lead to the activation of Ephrin(s) during somitogenesis: one is triggered by cMeso-1, and this pathway activates EphrinB2 through EphA4; and the other is by Tbx18 through unidentified Eph(s) to activate Ephrin(s) anteriorly. These multiple pathways operating in chickens contrast with those in mice, in which MesP2 is required for the intersomitic gap formation (3). Nevertheless, as no defects are seen in the somitic segmentation in any single knockout mice for Eph or Ephrin (15–17), it is possible that MesP2 regulates multiple Ephs in mice, which in turn interact with multiple Ephrins.

Eph-Ephrin signals are also known to be involved in the formation of an intersomitic gap in zebrafish (18). Contrasting with our findings in chickens, an Eph-forward signal is critical in zebrafish for the boundary formation with an Ephrin-reverse signal probably dispensable (18). Nonetheless, the importance of the Eph-forward signals for the epithelialization of posterior border cells is shared between chickens and zebrafish. The significance of the differences between the species in requirement of Ephrin-reverse and Eph-forward signals for the boundary formation remains unknown. They might reflect subtle differences in morphogenetic events during somitic segmentation: in chickens anterior border cells undergo MET before the posterior border cells whereas in zebrafish these cells epithelialize simultaneously upon border formation. Even though the precise mechanisms might differ from species to species, it should be emphasized that the framework of the molecular cascade that enables the intersomitic segregation appears to be conserved among vertebrate embryos with Eph-Ephrin signals playing a central role, the notice first proposed in 1992 by Nieto et al. (19).

Methods

Plasmids. pCAGGS-rtTA2^{S}-M2 and pTRE-EGFP (pBI-EGFP) were previously reported (7). A full-length cDNA of *DsRed-Express* (Clontech), chicken *EphA4* (20), chicken *EphA4ΔICD*, quail *Sox9* (21) or chick *Tbx18* (14) was subcloned into the pCAGGS expression vector (22). cDNA of human *CA-Cdc42* (23), human *NWASP-CRIB* (12), human *NWASP-CRIB-H208D* (24), *cMeso-1* (25), chicken *Pax2* (26), zebrafish *PAPC* (27), chicken *EphrinB2* (28), *EphrinB2ΔICD*, *EphrinB2ΔPDZb* or *EphrinB2FY* was inserted into blunt-ended MulI site of pTRE-EGFP. Mutant forms for EphA4 and EphrinB2 were generated by PCR using the following primers: EphA4ΔICD: 5′-ATGAAGCTGAATACAGAG-3′ (forward) and 5′-TCACTCATATGTAAAAGGATC-3′ (reverse), EphrinB2ΔICD: 5′-ATGGCAGCGCGGCGGCGCGACG-3′ (forward) and 5′-CTATCTTCTCCGGTACTTCAATAATAG-3′ (reverse), EphrinB2ΔPDZb: 5′-ATGGCAGCGCGGCGGCGCGACG-3′ (forward) and 5′-CTAGTAAATGTTTGCTGGACTCTGAGG-3′ (reverse). EphrinB2FY was constructed by the method of site-directed overhang extension PCR mutagenesis (29) with TRE-EprhinB2-EGFP as a template using following primers: 5′-ATGGCAGCGCGGCGGCGCGACG-3′ (1st PCR forward -I) and 5′-GAACACTGGATGTCCAAAGTCGCCGCTGACCTTTTCAAAGTGGGGGC-3′ (1st PCR reverse -I), 5′-CTTTGAAAAGGTCAGCGGCGACTTTGGACATCCAGTGTTCATAGTAC-3′ (1st PCR forward -II) and 5′-TCAGACCTTGTAGTAAATGTTTGCTGG-3′ (1st PCR reverse -II), 5′-ATGGCAGCGCGGCGGCGCGACG-3′ (2nd PCR forward) and 5′-TCAGACCTTGTAGTAAATGTTTGCTGG-3′ (2nd PCR reverse). *EphA4ΔICD* and *EphrinB2ΔICD* were manufactured as previously reported (18).

Embryonic Manipulations and *in Ovo* DNA Electroporation. Embryonic stages were determined according to Hamburger and Hamilton (30). *In ovo* DNA electroporation and embryonic manipulations were performed as previously described (1). The tet-on method was reported in Watanabe et al. (7). Microscopic images of dorsal views of developing embryos were obtained using Nikon SMZ7500 stereomicroscope equipped with a Zeiss AxioCam HRc CCD camera.

***In Situ* Hybridization.** A 473 bp-DNA fragment of chicken PAPC was obtained by RT-PCR using following primers: 5′-GACAGCGGCAAGGAGACAGTGATTTCAATGACAGTGACTCGG-3′ (forward) and 5′-CCAAGGAATGTGGTTGAGGGGCCGGGTAGAGGGGCACCCC-3′ (reverse).

Probe preparations were as described previously; *cMeso-1* (25), *Pax2* and *EphA4* (31), *Sox9* (21), *Tbx18* (14), and *EphrinB2* (28). *In situ* hybridization was performed as according to the methods of Nakaya et al. (6) and Sato et al. (1).

Confocal Microscopy. Embryos fixed in 4% paraformaldehyde (PFA)/PBS (PBS) were stained with Alexa Fluor 642 Phalloidin (Invitrogen) at 4 °C overnight. Confocal microscopic images were obtained using LSM 5 PASCAL confocal laser scanning microscope (Carl Zeiss). For three dimensional reconstruction, 15 slices of Z-section images (1 μm apart) were stacked by Zeiss LSM Examiner software. Paraffin sections of embryos were prepared using a microtome (MICROM, 178 HM325), and subjected to microscopy with Axioskop 2 Plus microscope (Carl Zeiss).

Immunohistochemistry. Embryos fixed in 4% PFA/phosphate-buffered saline (PBS) overnight were washed in 0.1% Triton in PBS (PBST) three times for 5 minutes each. The embryos were treated with 0.3% H_2O_2 in methanol for 1 hour and washed in PBST three times for 5 minutes each. After 1 hour of preblocking with 5% bovine serum albumin (BSA; fraction V) and 5% fetal bovine serum (FBS) in PBST, the embryos were incubated overnight at 4 °C with 1:1500 dilution of anti-phospho-EphrinB polyclonal antibody (rabbit; Cell Signaling) and 1:1000 dilution of anti-GFP polyclonal antibody (goat; Abcam) in 5% BSA/5% FBS/PBST. They were washed three times in PBST and incubated with EnVision anti-rabbit peroxidase polymer (Dako) and 1:500 dilution of anti-goat IgG-Alexa 488-conjugated antibody (donkey; Molecular Probes) for 30 minutes. After washing six times in TNT (0.1 M Tris-HCl (pH 7.5), 0.15 M NaCl, 0.1% Tween 20), the embryos were reacted with 1:200 dilution of Cy3-tyramid in 1×Amplification diluent (Perkin–Elmer) for 3 minutes at room temperature. The reaction was terminated by washing three times in TNT. Staining with anti-N-cadherin antibody was as described elsewhere (6).

Transfection of Cultured Cells and Western Blotting. Transfection of plasmids into DF-1 cells (32) was performed using Lipofectamin 2000 (Invitrogen). Two kinds of transfected cells were separately prepared: one with pCAGGS-rtTA2^{S}-M2 and pTRE-EphrinB2-EGFP, and the other with pCAGGS-EphA4 and pCAGGS-DsRed-E. After 24 hours these cells were co-cultured for further 12 hours in the presence of Dox (0.1 ng/μl) before harvested. For Western blotting analyses, the cells were treated in lysis buffer (50 mM Tris-HCl (pH 7.4), 10 mM $MgCl_2$, 1% Nonidet P-40, 100 mM NaCl, 10 mg/ml leupeptin, 10 mg/ml aprotinin, 10 mM (*p*-amidinophenyl)-methanesulfonyl fluoride). After centrifugation at 20,000 *g* for 4 minutes at 4 °C, the supernatant was suspended and boiled for 10 minutes in Laemmli sample buffer. The eluates were subjected to sodium dodecyl sulfate–polyacrylamide gel electrophoresis (SDS-PAGE), followed by immunoblotting with the anti-phospho-EphrinB polyclonal antibody (rabbit; Cell Signaling) and anti-GFP polyclonal antibody (rabbit; Molecular Probes) and horseradish peroxidase–conjugated anti-rabbit IgG antibody (Amersham). Signals were detected using the ECL Advance Western Blotting Detection kit (Amersham) by a luminous image analyzer LAS-3000 mini (Fuji Film).

ACKNOWLEDGMENTS. We thank S. Gilbert and D. Wilkinson for helpful discussion. We also thank A. Buchberger for *cMeso-1*, Dr. K. Ohta for *EphA4*, A. Yamamoto for *PAPC*, Y. Wakamatsu for *Sox9* and M. Tanaka and K. Tamura for *Tbx18*. This work was supported by a Grant-in-Aid for Scientific Research from the Ministry of Education, Culture, Sports, Science and Technology of Japan, and the Global COE program (Frontier Biosciences: Strategies for Survival and Adaptation in a Changing Global Environment), MEXT, Japan. Y.S. was a special postdoctoral researcher of RIKEN and also a Postdoctoral Fellow for Research Abroad of Japan Society for the Promotion of Science.

1. Sato Y, Yasuda K, Takahashi Y (2002) Morphological boundary forms by a novel inductive event mediated by Lunatic fringe and Notch during somitic segmentation. *Development* 129:3633–3644.
2. Takahashi Y, Sato Y (2008) Somitogenesis as a model to study the formation of morphological boundaries and cell epithelialization. *Dev Growth Differ* 50(Suppl 1):S149–S155.
3. Saga Y, Hata N, Koseki H, Taketo MM (1997) Mesp2: A novel mouse gene expressed in the presegmented mesoderm and essential for segmentation initiation. *Genes Dev* 11:1827–1839.
4. Takahashi Y, Kitajima S, Inoue T, Kanno J, Saga Y (2005) Differential contributions of Mesp1 and Mesp2 to the epithelialization and rostro-caudal patterning of somites. *Development* 132:787–796.
5. Yasuhiko Y et al. (2006) Tbx6-mediated Notch signaling controls somite-specific Mesp2 expression. *Proc Natl Acad Sci USA* 103:3651–3656.
6. Nakaya Y, Kuroda S, Katagiri YT, Kaibuchi K, Takahashi Y (2004) Mesenchymal-epithelial transition during somitic segmentation is regulated by differential roles of Cdc42 and Rac1. *Dev Cell* 7:425–438.
7. Watanabe T et al. (2007) Tet-on inducible system combined with *in ovo* electroporation dissects multiple roles of genes in somitogenesis of chicken embryos. *Dev Biol* 305:625–636.
8. Kitajima S, Takagi A, Inoue T, Saga Y (2000) MesP1 and MesP2 are essential for the development of cardiac mesoderm. *Development* 127:3215–3226.
9. Kalo MS, Yu HH, Pasquale EB (2001) In vivo tyrosine phosphorylation sites of activated ephrin-B1 and ephB2 from neural tissue. *J Biol Chem* 276:38940–38948.
10. Torres R et al. (1998) PDZ proteins bind, cluster, and synaptically colocalize with Eph receptors and their ephrin ligands. *Neuron* 21:1453–1463.
11. Cowan CA, Henkemeyer M (2001) The SH2/SH3 adaptor Grb4 transduces B-ephrin reverse signals. *Nature* 413:174–179.
12. Miki H, Sasaki T, Takai Y, Takenawa T (1998) Induction of filopodium formation by a WASP-related actin-depolymerizing protein N-WASP. *Nature* 391:93–96.
13. Takenawa T, Miki hours (2001) WASP and WAVE family proteins: key molecules for rapid rearrangement of cortical actin filaments and cell movement. *J Cell Sci* 114:1801–1809.
14. Tanaka M, Tickle C (2004) Tbx18 and boundary formation in chick somite and wing development. *Dev Biol* 268:470–480.
15. Davy A, Soriano P (2007) Ephrin-B2 forward signaling regulates somite patterning and neural crest cell development. *Dev Biol* 304:182–193.
16. Adams RH et al. (1999) Roles of ephrinB ligands and EphB receptors in cardiovascular development: Demarcation of arterial/venous domains, vascular morphogenesis, and sprouting angiogenesis. *Genes Dev* 13:295–306.
17. Orioli D, Henkemeyer M, Lemke G, Klein R, Pawson T (1996) Sek4 and Nuk receptors cooperate in guidance of commissural axons and in palate formation. *EMBO J* 15:6035–6049.
18. Barrios A et al. (2003) Eph/Ephrin signaling regulates the mesenchymal-to-epithelial transition of the paraxial mesoderm during somite morphogenesis. *Curr Biol* 13:1571–1582.
19. Nieto MA, Gilardi-Hebenstreit P, Charnay P, Wilkinson DG (1992) A receptor protein tyrosine kinase implicated in the segmental patterning of the hindbrain and mesoderm. *Development* 116:1137–1150.
20. Ohta K, et al. (1996) The receptor tyrosine kinase, Cek8, is transiently expressed on subtypes of motoneurons in the spinal cord during development. *Mech Dev* 54:59–69.
21. Sakai D, Suzuki T, Osumi N, Wakamatsu Y (2006) Cooperative action of Sox9, Snail2 and PKA signaling in early neural crest development. *Development* 133:1323–1333.
22. Momose T et al. (1999) Efficient targeting of gene expression in chick embryos by microelectroporation. *Dev Growth Differ* 41:335–344.
23. Kuroda S, et al. (1998) Role of IQGAP1, a target of the small GTPases Cdc42 and Rac1, in regulation of E-cadherin-mediated cell-cell adhesion. *Science* 281:832–835.
24. Ono Y, et al. (2000) Two actions of frabin: direct activation of Cdc42 and indirect activation of Rac. *Oncogene* 19:3050–3058.
25. Buchberger A, Seidl K, Klein C, Eberhardt H, Arnold HH (1998) cMeso-1, a novel bHLH transcription factor, is involved in somite formation in chicken embryos. *Dev Biol* 199:201–215.
26. Okafuji T, Funahashi J, Nakamura H (1999) Roles of Pax-2 in initiation of the chick tectal development. *Brain Res Dev Brain Res* 116:41–49.
27. Yamamoto A, et al. (1998) Zebrafish paraxial protocadherin is a downstream target of spadetail involved in morphogenesis of gastrula mesoderm. *Development* 125:3389–3397.
28. Sato Y, et al. (2008) Notch mediates the segmental specification of angioblasts in somites and their directed migration toward the dorsal aorta in avian embryos. *Dev Cell* 14:890–901.
29. Ho SN, Hunt HD, Horton RM, Pullen JK, Pease LR (1989) Site-directed mutagenesis by overlap extension using the polymerase chain reaction. *Gene* 77:51–59.
30. Hamburger V, Hamilton HL (1992) A series of normal stages in the development of the chick embryo. 1951. *Dev Dyn* 195:231–272.
31. Suetsugu R, Sato Y, Takahashi Y (2002) Pax 2 expression in mesodermal segmentation and its relationship with EphA4 and Lunatic-fringe during chicken somitogenesis. *Mech Dev* 119(Suppl 1):S155–S159.
32. Himly M, Foster DN, Bottoli I, Iacovoni JS, Vogt PK (1998) The DF-1 chicken fibroblast cell line: transformation induced by diverse oncogenes and cell death resulting from infection by avian leukosis viruses. *Virology* 248:295–304.